Ab initio study of one- and two-electron transfer processes in collisions of Ne^{2+} with He at low to intermediate energies

T. W. Imai and M. Kimura
Graduate School of Science and Engineering and Center for Plasma Material Sciences, Yamaguchi University, Ube, Yamaguchi 755-8611, Japan

J. P. Gu, G. Hirsch,* and R. J. Buenker
Theoretische Chemie, Bergische Universität Wuppertal, D-42097 Wuppertal, Germany

J. G. Wang and P. C. Stancil
Department of Physics and Astronomy and the Center for Simulational Physics, The University of Georgia, Athens, Georgia, 30602-2451, USA

Lukas Pichl
Department of Computer Software, University of Aizu, Aizu-Wakamatsu, Fukushima 965-8580, Japan
(Received 11 February 2002; revised manuscript received 5 March 2003; published 24 July 2003)

One- and two-electron-transfer processes resulting from Ne^{2+} collisions with He are studied, based on a molecular-orbital close-coupling method within the semiclassical representation for the collision energy range of 10 eV/u–10 keV/u. One-electron processes are considered from ground state $Ne^{2+}(^3P)$ as well as from the metastable ions $Ne^{2+}(^1D)$ and $Ne^{2+}(^1S)$. Two-electron processes are considered only for metastable $Ne^{2+}(^1D)$ and $Ne^{2+}(^1S)$ collisions. Previous electron-transfer experimental cross sections show a weak energy dependence, while the present theoretical results for the ground-state ion impact have a pronounced energy dependence, decreasing with decreasing collision energy. However, the theoretical cross sections for the metastable ions are found to be weakly dependent on the collision energy. If the ion beams used in the experiments are assumed to have contained some fraction of metastable ions, then the present results appear to be consistent with the measurements.

DOI: 10.1103/PhysRevA.68.012716 PACS number(s): 34.70.+e, 34.10.+x

I. INTRODUCTION

The investigations of ion-atom collisions are important not only for fundamental physical research, but also in applied fields. Examples include astrophysics, radiology, and ion-beam interactions with surfaces for ion implantation and thin-film manufacturing. In many astrophysical environments, Ne^{2+} and Ne^{+} ions are known to be abundant, and the electron-capture processes in collisions with H and He atoms may play a role in the ionization balance [1]. In heavy-ion radiation therapy, bombarding ions result in ionization and electron capture from biomolecules as well as water molecules dominantly present in human cells, hence inducing destruction of cancerous cells and tumors. Neon ions are considered to be one of the strong candidates for use in the future as an ion source for effective treatment. Therefore, it is necessary to have a fundamental understanding of the microscopic dynamics of atomic collision reactions for neon ions and to provide accurate electron-transfer cross sections for a wide range of collision energies.

In this paper, we report on *ab initio* investigations of one- and two-electron transfer in $^{20}Ne^{2+}$ collisions with He for collision energies between 10 eV/u and 10 keV/u. The processes we are interested in are for the ground-state neon ion (through the triplet manifold),

$$Ne^{2+}(^3P)+He(^1S)\rightarrow Ne^{+}(^2P^o)+He^{+}(^2S), \quad (1)$$

and for the metastable ions (through the singlet manifold),

$$Ne^{2+}(^1D)+He(^1S)\rightarrow Ne^{+}(^2P^o,2D,^2S)+He^{+}(^2S), \quad (2)$$

$$Ne^{2+}(^1S)+He(^1S)\rightarrow Ne^{+}(^2P^o,^2D,^2S)+He^{+}(^2S). \quad (3)$$

For the triplet manifold, charge transfer from ground state $Ne^{2+}(^3P)$ is expected to be dominated by the exoergic process (1). While capture can proceed to excited states, the lowest available channel is endoergic by 10.53 eV (3.156 eV/u). They are expected to contribute at relatively high energies and are not considered here. For the singlet manifold, several excited states are available within a few eV (>3.656 eV or 1.1 eV/u), which can be reached for the present considered collision energies. Therefore, for the singlet manifold, captures to the endoergic ^2D and ^2S channels are also included.

While there are five experimental investigations [2–6] of the electron transfer for this system in the collision energy region of interest, we are unaware of any theoretical scattering calculations. However, molecular structure calculations, of essentially the same states considered in this work, have been performed by Mercier *et al.* [7] and Ben-Itzhak *et al.* [8]. Mercier *et al.* calculated the diabatic potential curves, including the two-electron-transfer $[Ne(^1S)+He^{2+}]$ channel, and found that the diabatic potential curves for the initial

*Deceased.

and the final channels in reactions (1)–(3) cross at short internuclear distances less than $3a_0$, and hence, suggested that double capture might play an important role as an intermediary for capture to the excited $Ne^+(^2S)$ state from $Ne^{2+}(^1D)$ and $Ne^{2+}(^1S)$. Experimental studies are reported by Suk *et al.* [2] for energies from 3 to 10 keV/u, Bloemen *et al.* [3] from 1 to 20 keV/u, Kusakabe *et al.* [5] from 0.15 to 1.2 keV/u, Okuno and Kaneko [4] from 5 to 180 eV/u, and Flaks and Solov'ev [6] from 0.6 to 2.5 keV/u. The experimental cross sections are found to show a gradual increase above 0.5 keV/u with a magnitude of $(1-2)\times10^{-16}$ cm^2. The data of Kusakabe *et al.* [5] and Okuno and Kaneko [4] are found to agree well with each other throughout their overlapping energy region. From 150 to 10 eV/u, the results of Okuno and Kaneko are almost energy independent with a value of 2×10^{-17} cm^2, followed by a nearly step-function-like drop below 10 eV/u. The energy separation between the ground $Ne^{2+}(^3P)$ and the excited $Ne^{2+}(^1D)$ states is merely 3.2 eV, suggesting that it is possible that the ion beams used in these experiments might contain some fraction of metastable ions. We will investigate this possibility since it is usually the case that ground and excited ions behave quite differently, resulting in completely distinct dynamics and cross sections [9]. We also investigate two-electron-transfer processes,

$$Ne^{2+}(^1D)+He(^1S)\rightarrow Ne(^1S)+He^{2+} \tag{4}$$

and

$$Ne^{2+}(^1S)+He(^1S)\rightarrow Ne(^1S)+He^{2+}. \tag{5}$$

The two-electron-transfer $[Ne(^1S)+He^{2+}]$ state considered here belongs only to the singlet manifold, and therefore the triplet manifold is excluded. The experimental data for double-electron capture are reported by Kusakabe *et al.* [5] from 0.15 to 1.2 keV/u and by Flaks and Solov'ev [6] from 0.3 to 3 keV/u. The data of Kusakabe *et al.* [5] increase rapidly as the collision energy increases with values of $1.97\times10^{-18}-1.17\times10^{-17}$ cm^2, while those of Flaks and Solov'ev [6] also increase with the increasing collision energy varying from 8×10^{-18} cm^2 to 3×10^{-17} cm^2. The double-capture-cross sections are nearly an order of magnitude smaller than those of single capture. It is interesting to relate this result to the claim of Mercier *et al.* [7] that the double-capture channel plays an important role as an intermediary for single capture.

II. THEORETICAL MODEL

A. Molecular states

The adiabatic potential energies and the molecular wave functions of $NeHe^{2+}$ are obtained by employing the *ab initio* multireference single- and double-excitation configuration interaction (MRD-CI) method [10] with configuration selection at a threshold of 1.0×10^{-7} a.u. and energy extrapolation, using the TABLE CI algorithm [11]. The two electrons in the first (lowest) molecular orbital (MO) are kept inactive in the present CI calculation, and the highest MO is discarded. The coupling matrix elements are calculated using the resulting CI wave functions. The radial coupling matrix elements are obtained using a finite-difference method [12]. In the calculation for the Ne atom, the cc-pVQZ correlation-consistent, polarization valence, quadruple zeta basis set [13] is used, but the g function in this basis set is discarded. In addition to the above basis set, several diffuse functions are added. The basis set for the neon atom is thus $(14s8p3d2f)$, contracted to $[7s6p3d2f]$. For the helium atom, the $(7s3p)/[5s3p]$ basis set in Ref. [14] is employed and one *d*-type function with an exponent of 1.0 was added. Further details of the *ab initio* MRD-CI calculations are listed in Table I.

TABLE I. Number of reference configurations, N_{ref}, and number of roots, N_{root}, treated in each irreducible representation and the corresponding number of generated (N_{tot}) and selected (N_{sel}) symmetry-adapted functions for a threshold of 1.0×10^{-7} a.u. at an internuclear distance of $2.3a_0$ for the $HeNe^{2+}$ system.

State	N_{ref}/N_{root}	N_{tot}	N_{sel}
$^2A_1$	45/5	751978	163969
$^2B_1$	32/5	753895	158506
$^2A_2$	22/3	689178	99571
$^4B_1$	19/4	518004	134716
$^4A_2$	23/3	596143	111147
Singlets	N_{ref}/N_{root}	N_{tot}	N_{sel}
A_1	68/5	623256	154650
B_1/B_2	29/3	631087	148365
A_2	36/2	514872	101296
Triplets	N_{ref}/N_{root}	N_{tot}	N_{sel}
A_1	52/2	547252	142386
B_1/B_2	30/3	561350	146502
A_2	27/2	512256	98258

B. Scattering dynamics

In the semiclassical impact parameter close-coupling (CC) method [15], the relative motion of the projectile nucleus is treated classically with a straight-line trajectory, while the electronic motion is treated quantum mechanically. The total wave function of the collision system is expanded in terms of adiabatic molecular eigenfunctions. By substituting the total wave function into the time-dependent Schrödinger equation, coupled equations as a function of time are obtained. All radial and rotational coupling matrix elements among the molecular states considered are included in the present calculations. The transition amplitudes can be obtained by solving the coupled equations. By integration of the square of the transition amplitudes over the impact parameter, the cross sections are determined.

In the current calculations, two sets of channels were considered: (i) for the triplet manifold, where four molecular states with the initial $[Ne^{2+}(^3P)+He(^1S)]$ and the final $[Ne^+(^2P^o)+He^+(^2S)]$ states in Eq. (1) were included (4-MOCC), and (ii) for the singlet manifold for processes (2) through (5), eight states with the initial $[Ne^{2+}(^1D,^1S)+He(^1S)]$ and final one-electron-transfer $[Ne^+(^2P^o,^2D,^2S)+He^+(^2S)]$ states, in addition to the two-

TABLE II. The $NeHe^{2+}$ molecular states considered.

Molecular state	Separated atom	Relative energy (cm^{-1})
$1\ ^3\Sigma^+, 1\ ^3\Pi$	$Ne^+(2s^2 2p^5\ ^2P^o) + He^+(1s\ ^2S)$	0
$1\ ^1\Sigma^+, 1\ ^1\Pi$		
$1\ ^3\Sigma^-, 2\ ^3\Pi$	$Ne^{2+}(2s^2 2p^4\ ^3P) + He(1s^2\ ^1S)$	133045
$2\ ^1\Sigma^+, 2\ ^1\Pi$	$Ne^{2+}(2s^2 2p^4\ ^1D) + He(1s^2\ ^1S)$	158886
$3\ ^1\Sigma^+$	$Ne^{2+}(2s^2 2p^4\ ^1S) + He(1s^2\ ^1S)$	188792
$4\ ^1\Sigma^+$	$Ne^+(2s 2p^6\ ^2S) + He^+(1s\ ^2S)$	217050
$5\ ^1\Sigma^+$	$Ne^+(2s^2 2p^4 3s\ ^2D) + He^+(1s\ ^2S)$	247886
$6\ ^1\Sigma^+$	$Ne(2s^2 2p^6\ ^1S) + He^{2+}(^1S)$	258854

electron-transfer $[Ne(^1S) + He^{2+}]$ state, are considered (8-MOCC). Because spin-orbit coupling should be negligibly small compared to radial and rotational coupling in the present energy region, mixing of the triplet and singlet manifolds is not included in the calculations.

The semiclassical MOCC method is generally applicable for the range of collision energies considered in this study. However, the method may have some problems at the two extremes. At the lowest energies, the use of the straight-line trajectories may not be reliable (see more below). At the highest energy of 10 keV/u, the contribution to the total cross sections from the additional excited states is expected to increase. Further, the neglect of the electron translation factors and the ionization channel may be of some concern but, as we will see below, the agreement between the current calculations and the available experiments is quite good at the highest energies.

III. RESULTS AND DISCUSSION

A. Adiabatic potentials and coupling matrix elements

All considered molecular states of the $NeHe^{2+}$ system are listed in Table II. The adiabatic potential curves as a function of the internuclear distance R are shown graphically in Fig. 1. Among all molecular states, the $[Ne^+(^2P^o) + He^+(^2S);\ 1\ ^1\Sigma^+, 1\ ^1\Pi, 1\ ^3\Sigma^+$, and $1\ ^3\Pi]$ channels are energetically the lowest. $[Ne^{2+}(^3P) + He(^1S);\ 1\ ^3\Sigma^-$ and $2\ ^3\Pi]$ correspond to the initial ground-state charge-transfer channels, while $[Ne^{2+}(^1D) + He(^1S);\ 2\ ^1\Sigma^+$ and $2\ ^1\Pi]$ and $[Ne^{2+}(^1S) + He(^1S);\ 3\ ^1\Sigma^+]$ are the initial metastable charge-transfer channels. The $[Ne^+(^2S) + He^+(^2S);\ 4\ ^1\Sigma^+]$, $[Ne^+(^2D) + He^+(^2S);\ 5\ ^1\Sigma^+]$, and $[Ne(^1S) + He^{2+};\ 6\ ^1\Sigma^+]$ states all lie higher in energy than the metastable $[Ne^{2+}(^1S) + He(^1S)]$ state. Mercier *et al.* presented quasidiabatic potentials which were obtained based on their CI calculations, but they ignored those states which lead to the $[Ne^+(^2S) + He^+(^2S)]$ and $[Ne^+(^2D) + He^+(^2S)]$ channels. They found the diabatic $[Ne(^1S) + He^{2+}]$ channel to be the lowest state for internuclear distances less than $2a_0$ due to a series of crossings with many other states. Hence, they concluded that the $[Ne(^1S) + He^{2+}]$ state should play an important role in the electron-transfer dynamics. In our more rigorous molecular-orbital calculations, we included not only the $[Ne(^1S) + He^{2+}]$ state but also the intermediate $[Ne^+(^2S) + He^+(^2S)]$ and $[Ne^{2+}(^2D) + He^+(^2S)]$ states and performed the computation in the adiabatic representation. Our results indicate that there are no strong avoided crossings at short internuclear distances between the $4\ ^1\Sigma^+$ and low-lying states, which would be necessary to produce the behavior of the diabatic $[Ne(^1S) + He^{2+}]$ channel found by Mercier *et al.* This is further confirmed by the molecular-orbital calculations of Ben-Itzhak *et al.* [8], which are very similar to those presented in this work.

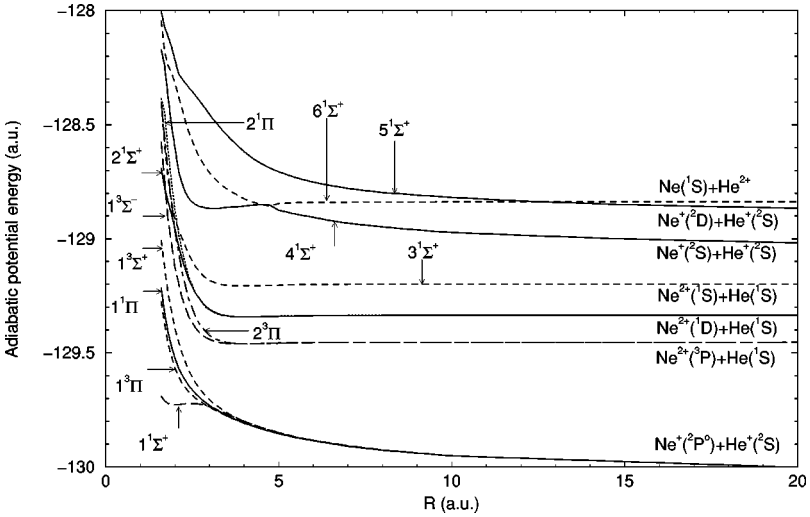

FIG. 1. Adiabatic potentials of the considered $HeNe^{2+}$ molecular states.

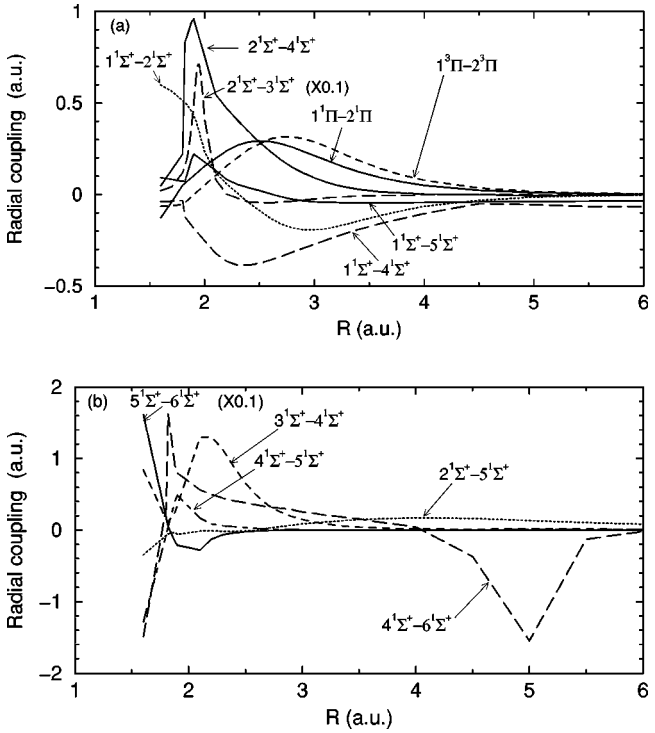

FIG. 2. Radial coupling matrix elements of $NeHe^{2+}$.

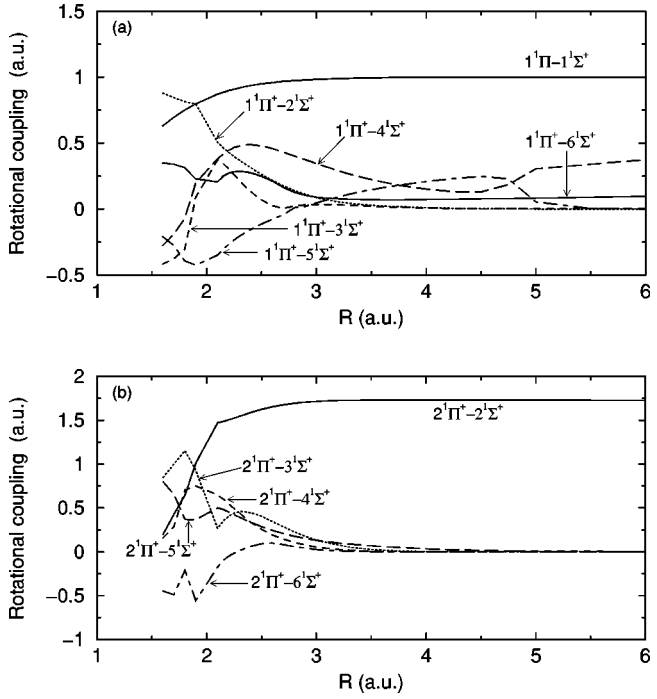

FIG. 3. Rotational coupling matrix elements of $NeHe^{2+}$.

Figure 2 displays representative radial coupling matrix elements. The $5\ ^1\Sigma^+ - 6\ ^1\Sigma^+$ matrix element has a peak near $2a_0$, and rapidly approaches zero for larger internuclear separations. It is the only route by which the $Ne^+(^2D)$ state can be populated as the crossing between the $5\ ^1\Sigma^+$ and $6\ ^1\Sigma^+$ states near $12a_0$ is treated diabatically. The large $4\ ^1\Sigma^+ - 6\ ^1\Sigma^+$ radial coupling peak near $5a_0$ determines the relative populations for double capture and single capture into $Ne^+(^2S)$. The radial coupling matrix element for the triplet manifold, $1\ ^3\Pi - 2\ ^3\Pi$, is small in magnitude with a broad peak located at an internuclear distance of $\sim 2.5a_0$. Figure 3 shows representative rotational coupling matrix elements. The couplings for $1\ ^1\Pi - 4\ ^1\Sigma^+, -5\ ^1\Sigma+$, and $-6\ ^1\Sigma^+$ are weak, and have small and broad peaks below $5a_0$. They all decrease quickly approaching zero with increasing R. The rotational matrix elements that are finite at large R couple with molecular states which are degenerate in the separated-atom limit.

B. One-electron transfer in Ne^{2+}+He collisions

We have investigated process (1) considering four channels in the triplet manifold (4-MOCC), and processes (2) and (3) in the singlet manifold including a maximum of eight channels (8-MOCC). These calculations constitute the results that are presented here. However, we have performed some cursory convergence studies for the singlet manifold by repeating the scattering calculations and neglecting the high-lying $4\ ^1\Sigma^+$, $5\ ^1\Sigma^+$, and $6\ ^1\Sigma^+$ states. As the number of high-lying channels is increased, the capture cross section to the ground state $Ne^+(^2P^o)$ decreases. However, this effect depends strongly on the collision energy increasing with the energy. While this is not a comprehensive convergence study, which is not readily performed with the MOCC method, the number of included states for the singlet manifold (8-MOCC) are believed to be sufficient to provide accurate cross sections. The inclusion of even higher-lying states, which are even more endoergic, will only be relevant for the highest considered collision energies and above.

1. Ground-state $Ne^{2+}(^3P)$ ion impact

The partial and total single-electron capture cross sections for process (1) are shown in Fig. 4 from the triplet-manifold (4-MOCC) calculation. As described above, within the present model only capture to $Ne^+(^2P^o)$ is considered. The

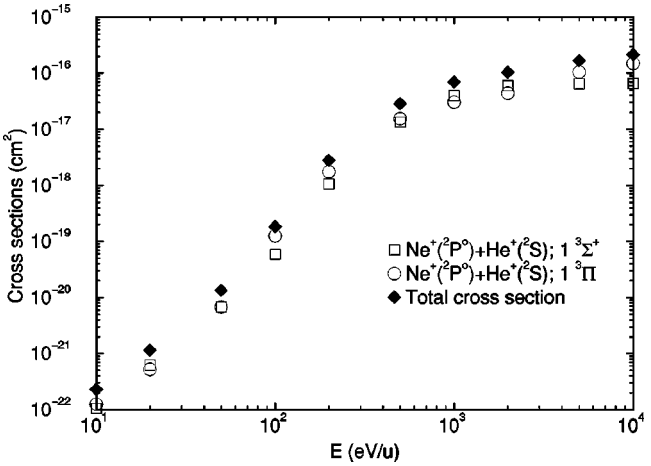

FIG. 4. One-electron-transfer cross sections for $Ne^{2+}(^3P)+He(^1S)$ collisions. Open squares indicate the final $1\ ^3\Sigma^+$ state, open circles the $1\ ^3\Pi$ state, and filled diamonds the total transfer cross section.

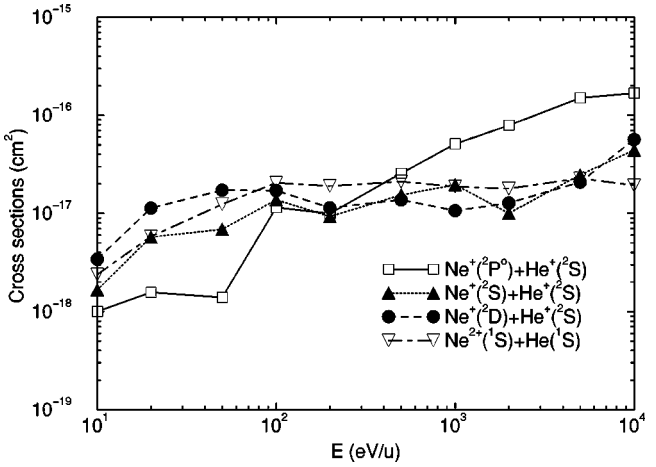

FIG. 5. One-electron-transfer and excitation cross sections for $Ne^{2+}(^1D)+He(^1S)$ collisions. Electron transfer: $Ne^+(^2P^o)+He^+(^2S)$ formation (open squares); $Ne^+(^2S)+He^+(^2S)$ formation (filled triangles, up); $Ne^+(^2D)+He^+(^2S)$ formation (filled circles). Excitation: $Ne^{2+}(^1S)+He(^1S)$ formation (open triangles, down).

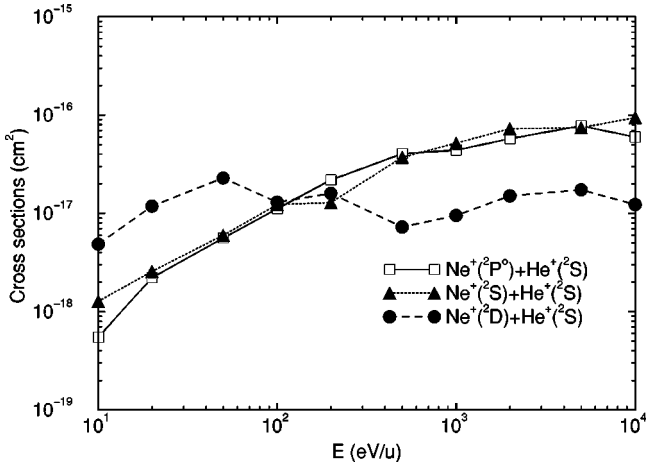

FIG. 6. One-electron-transfer cross sections of $Ne^{2+}(^1S)+He(^1S)$ collisions. $Ne^+(^2D)+He^+(^2S)$ formation (filled circles); $Ne^+(^2S)+He^+(^2S)$ formation (filled triangles, up); $Ne^+(^2P^o)+He^+(^2S)$ formation (open squares).

cross sections increase rapidly up to 1 keV/u before leveling off. The figure displays an oscillation pattern between the partial cross sections for capture to the $1\ ^3\Pi$ and $1\ ^3\Sigma^+$ states. However, this oscillation is weak, with the magnitudes of Ne^+ production through the $1\ ^3\Sigma^+$ and $1\ ^3\Pi$ channels being nearly equal over the entire energy range considered. This might at first appear to be surprising since the $1\ ^3\Pi$ channel is populated by both radial and rotational couplings, while $1\ ^3\Sigma^+$ can only be accessed through rotational coupling. However, as there are no strong avoided crossings between the entrance and the exit channels, radial coupling is not very effective. This feature, which is a consequence of the large exoergic energy defect of 16 eV, also explains why the cross section decreases rapidly with decreasing collision energy.

2. Metastable $Ne^{2+}(^1D)$ and $Ne^{2+}(^1S)$ ion impact

The partial cross sections for capture to $Ne^+(^2P^o)$, $Ne^+(^2S)$, and $Ne^+(^2D)$ through processes (2) and (3) are shown in Figs. 5 and 6, respectively, from the singlet-manifold (8-MOCC) calculation. For $Ne^{2+}(^1D)$ collisions with $He(^1S)$ in Fig. 4, the $Ne^+(^2S)$ and $Ne^+(^2D)$ capture cross sections are very similar in magnitude and in general shape as a function of energy. This suggests strong mixing of the flux between these two levels, attributable to the $5\ ^1\Sigma^+ - 6\ ^1\Sigma^+$ coupling. Both cross sections are fairly flat throughout the considered energy range, but begin to decrease below $\sim$50 eV/u. The low energy decrease appears to be consistent with the thresholds of 2.21 and 3.30 eV/u for capture to $Ne^+(^2S)$ and $Ne^+(^2D)$, respectively. The cross section for capture to $Ne^+(^2P^o)$ is smaller than the cross sections for $Ne^+(^2D)$ and $Ne^+(^2S)$ by a factor of 2 or more below 100 eV/u, although it is the dominant channel for higher energies. All three partial cross sections display oscillatory behavior due to multichannel interference, but the mechanism is difficult to disentangle due to the large number of states involved. The oscillations between $Ne^+(^2S)$ and $Ne^+(^2D)$ with $Ne^+(^2P^o)$ appear to be out of phase. As noted for the triplet manifold, the Σ and Π contributions (not shown) to the appropriate channels are similar in magnitude.

For $Ne^{2+}(^1S)$ collisions with $He(^1S)$ as shown in Fig. 6, the partial cross-section amplitudes and oscillatory patterns are similar to those for $Ne^{2+}(^1D)$. The decrease in the capture cross sections below $\sim$50 eV/u, appears to be consistent with the thresholds of 1.1 and 2.2 eV/u for $Ne^+(^2S)$ and $Ne^+(^2D)$, respectively.

3. Comparison of one-electron-transfer cross sections with the experimental data

In Fig. 7, we compare the present theoretical cross sections with those of the experiments [2–6]. The single-electron-capture cross sections from ground state $Ne^{2+}(^3P)$ is seen to be in reasonable agreement with the measurements of Suk *et al.* and Bloemen *et al.*, with Kusakabe *et al.* above $\sim$1.3 keV/u, and with Flaks and Solov'ev above $\sim$0.6 keV/u. There is a significant discrepancy with the measurements of Okuno and Kaneko [4] and the lower-energy results of Kusakabe *et al.* [5] and Flaks and Solov'ev [6]. In particular, the present theoretical cross section for $Ne^{2+}(^3P)$ monotonically decreases as the collision energy decreases, while those of Okuno and Kaneko [4] are fairly flat from $\sim$10 to 200 eV/u. From the close inspection of the relevant potential curves and corresponding couplings, it is more natural to expect that the cross section for $Ne^{2+}(^3P)$ should display a decreasing trend with decreasing collision energy as obtained in the present calculations due to the relatively large energy defect and the lack of strong avoided crossings and correspondingly weak couplings.

It is possible that the current low-energy $Ne^{2+}(^3P)$ cross section is too small due to the neglect of the high-lying endoergic channels in the 4-MOCC calculation. Usually endoergic channels are found to only become significiant for energies above $\sim$0.1–1 keV/u, though this occurs when there is a dominant exoergic channel with an optimally located

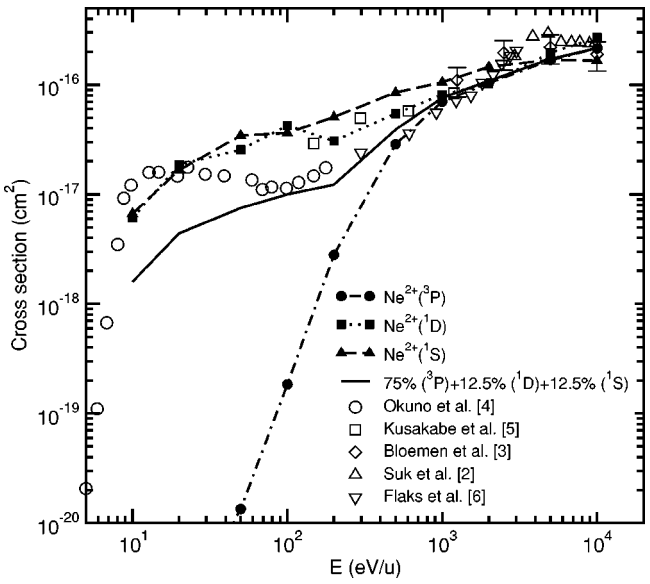

FIG. 7. Comparison of the present total one-electron-transfer cross sections with measurements. Theory: $Ne^{2+}(^3P)$ (dotted-dashed line); $Ne^{2+}(^1D)$ (dotted line); $Ne^{2+}(^1S)$ (long dashed line); 75% $Ne^{2+}(^3P)+12.5\%$ $Ne^{2+}(^1D)+12.5\%$ $Ne^{2+}(^1S)$ (solid line). Experiments: Suk *et al.* [2] (open triangles, up); Bloemen *et al.* [3] (open diamonds); Okuno and Kaneko [4] (open circles); Kusakabe *et al.* [5] (open squares); Flaks and Solov'ev [6] (open triangles, down).

avoided crossing (e.g., Refs. [16,17]). However, for the current case which lacks strong avoided crossings, capture for the metastable ions, displayed in Figs. 5 and 6, shows the endoergic and exoergic channels to have similar cross section magnitudes down to 10 eV/u approaching the endoergic thresholds. This suggests that the total $Ne^{2+}(^3P)$ cross section might be increased with the inclusion of endoergic channels. However, there are some important differences between the triplet-manifold potential curves for the ground state and those of the singlet manifold for the metastable ions. First, the minimum threshold for capture to $Ne^+(^2S)$ from a metastable state is 1.1 eV/u, while that from the ground state is 3.2 eV/u. Second, the molecular potential in the triplet manifold which correlates to $Ne^+(^2S)$ is completely repulsive (see the $e\ ^3\Sigma^+$ state given in Ref. [8]), while the corresponding state in the singlet manifold, $4\ ^1\Sigma^+$, is attractive for $R < 5a_0$ due to an interaction with the double-capture channel. Therefore, the effective threshold for the ground-state cross section is expected to be higher than that of 3.2 eV/u, due to the asymptotic energy differences only. Further, for energies less than ~50-100 eV/u, the straight-line trajectory approximation, adopted here for the current *semiclassical* MOCC calculations, might break down, which usually results in the semiclassical cross sections being too large (e.g., Ref. [18]). Finally, the state-selective measurements of Bloemen *et al.* [3] suggest that capture to the ground state $Ne^+(^2P^o)$ dominates the total one-electron-transfer cross section for $Ne^{2+}(^3P)$. A possible way to resolve these issues is to perform a *quantum-mechanical* MOCC calculation for the triplet manifold with inclusion of endoergic channels. Such calculations will be the subject of a subsequent publication. However, the current semiclassical MOCC calculations for single capture are sufficient to suggest that most, if not all, of the neon ion beams contained some fraction of metastable ions. We now consider the influence the metastable ions might have on the measured charge-transfer cross sections.

The present total charge-transfer cross sections for the metastable $Ne^{2+}(^1D)$ and $Ne^{2+}(^1S)$ ions are relatively large, as can be seen in Figs. 5 and 6 for the partial cross sections and displayed in Fig. 7 for the total cross sections. The general slope of the metastable cross sections is much smaller than that of the ground state, the cross section decreases slowly as the collision energy is lowered. In fact, the present results for either metastable ions are in good accord with nearly all of the measurements over the entire energy region studied, though usually somewhat larger. If we assume that the ion beams used in the experiments contain some fraction of metastable ions, a reasonable agreement with the measured cross sections can be obtained by arbitrarily adopting a mixing fraction of 75% $Ne^{2+}(^3P)$ and 25% metastable with equal fractions of each metastable ion. The resulting mixed cross section, shown in Fig. 7, agrees with all of the experiments for $E \gtrsim 70$ eV/u, but falls significantly below the results of Okuno and Kaneko for smaller collision energies. Although all of the experimental studies intended to carry out ground-state $Ne^{2+}(^3P)$ ion measurements, they did not exclude the possibility of some metastable contamination of their ion beams. Our estimated value of a 25% metastable contamination might seem large, but metastable ions can easily be produced in typical ion sources as the ^1D and ^1S states are only 3.2 and 6.9 eV, respectively, above the ground state. Even if the current semiclassical MOCC calculations for $Ne^{2+}(^3P)$ underestimate the true cross section due to the neglect of endoergic channels, it would seem very difficult to understand the behavior of the cross section below 50 eV/u measured by Okuno and Kaneko. The finite cross section measured at 5 eV/u is uncomfortably close to the endoergic, separated-atom threshold of 3.2 eV/u.

4. Projectile-ion excitation to $Ne^{2+}(^1S)$

Figure 5 also displays the $Ne^{2+}(^1D) \rightarrow Ne^{2+}(^1S)$ excitation cross section due to collisions with He. It is weakly energy dependent with a few fluctuations over the considered energy range. Apparently, these oscillations are due to multichannel interferences as they are similar in nature to the noted oscillations in the charge-transfer cross sections. The magnitude of the excitation cross section is comparable to that of charge transfer, indicating that it might play a role for flux promotion to higher-lying charge-transfer states. If the He density is large enough such that multiple collision events occur, then additional $Ne^{2+}(^1S)$ metastable ions can be produced in the beam from $Ne^{2+}(^1D)$ through this mechanism, which has a threshold of only 1.1 eV/u.

C. Two-electron transfer in Ne^{2+}+He collisions

In this section, we consider the two-electron-transfer processes (4) and (5) which occur only through the singlet manifold, i.e., for collisions of the metastable ions. Double cap-

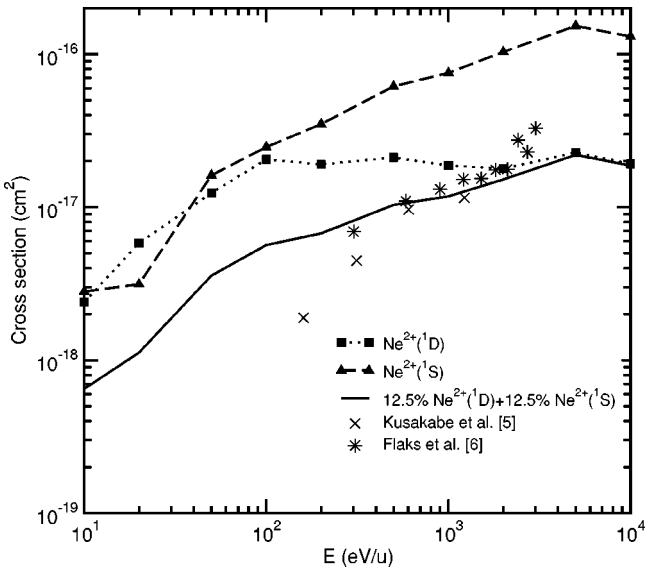

FIG. 8. Comparison of the present total double-capture cross sections with measurements. Theory: $Ne^{2+}(^1D)$ (dotted line); $Ne^{2+}(^1S)$ (long dashed line); 12.5% $Ne^{2+}(^1D)$ +12.5% $Ne^{2+}(^1S)$ (solid line). Experiments: Kusakabe *et al.* [5]; Flaks and Solov'ev [6].

ture from ground state Ne^{2+} occurs only through the triplet manifold and only into excited Ne states with the lowest threshold being 9.9 eV/u (or 16.6 eV above the highest state treated in the present molecular-orbital calculations), and is not considered here. The thresholds for double capture from $Ne^{2+}(^1D)$ and $Ne^{2+}(^1S)$ to the Ne ground state are 2.87 and 3.98 eV/u, respectively. Figure 8 depicts the cross sections for two-electron transfer for ^1D and ^1S. Both are of similar magnitude for energies less than 100 eV/u and display some interference behavior. There appear to be interactions between the $2\ ^1\Sigma^+ \rightarrow 6\ ^1\Sigma^+$, and $2\ ^1\Sigma^+ \rightarrow 5\ ^1\Sigma^+$ transitions, between the $2\ ^1\Pi \rightarrow 6\ ^1\Sigma^+$ and $2\ ^1\Pi \rightarrow 4\ ^1\Sigma^+$ transitions, and between the $3\ ^1\Sigma^+ \rightarrow 6\ ^1\Sigma^+$, and $3\ ^1\Sigma^+ \rightarrow 4\ ^1\Sigma^+$ transitions. The computed cross sections have energy dependencies similar to the single charge-tranfer results for the metastable ions, decreasing with decreasing energy towards their threshold. The available experimental data for the two-electron transfer from Kusakabe *et al.* [5] and Flaks and Solov'ev [6] are generally smaller than found in the current calculations, but agree well with each other. The energy dependence of the experimental data is similar to our result for $Ne^{2+}(^1S)$, but nearly an order of magnitude smaller. The experiments assumed that the cross sections depict double capture from the Ne^{2+} ground state, but it is likely, as we argued above for the single-electron capture, that the Ne ion beams have some fraction of metastable ions. Further, double capture from the ground state is far more endoergic than from the metastables, suggesting that the metastable cross sections should be larger for the considered energy range. If we assume the same fraction of metastable ions in the beam (25%) as deduced for single capture, we find as shown in Fig. 8 that our metastable cross sections are in good agreement with the measured values. This suggestion that the majority of the measured double-capture cross section magnitude is actually due to the metastable ions and not the ground state. While the experimental conditions of each of the measurements are surely different, it seems very likely that the beams contain metastable ions. The ability of the calculated double-electron-capture cross sections to reproduce the experiments is an additional piece of evidence for metastable contamination.

IV. SUMMARY

We have investigated one- and two-electron-transfer processes for $Ne^{2+}(^3P,^1D,^1S)$ collisions with He for collision energies between 10 eV/u and 10 keV/u within the semiclassical molecular-orbital close-coupling approach. Single-electron capture by ground state $Ne^{2+}(^3P)$ is a weak process at low energies, but becomes significant with increasing energy. On the contrary, one-electron transfer for metastable $Ne^{2+}(^1D)$ and $Ne^{2+}(^1S)$ is relatively large over the entire energy range studied. There are significant discrepancies between the present results for ground-state Ne^{2+} collisions and experimental data for energies less than 600 eV/u, where the theoretical result decreases rather sharply with decreasing energy, while the experimental data of Okuno and Kaneko [4] and Kusakabe *et al.* [5] have nearly a constant value. However, if one makes the reasonable speculation that there is a mixture of the ground and metastable Ne^{2+} ions in the experimental ion beams, then reasonable agreement is obtained. Indeed, if one assumes that the ion beam contains 75% of ground state $Ne^{2+}(^3P)$ and 12.5% each of $Ne^{2+}(^1D)$ and $Ne^{2+}(^1S)$, then the theoretical electron-transfer cross sections are found to be in good accord with these measurements for energies between 70 eV/u and 10 keV/u. Although further thorough experimental and theoretical study on this system for this energy region is desirable to resolve this uncertainty, we tentatively conclude that this is the case. We also present results for double-electron capture for metastable $Ne^{2+}(^1D,^1S)$ collisions for the same energy region, in which only the singlet manifold plays a role. If the same metastable fraction is assumed, good agreement is found with the measurements, providing further evidence for metastable contamination of the experimental ion beams, but also suggesting that the measured double-capture cross sections are primarily due to the metastable ions and not the ground state.

ACKNOWLEDGMENTS

The authors thank Dr. T. Kusakabe and Dr. K. Okuno for various useful discussions. The work was supported in part by the Grant-in-Aid, the Ministry of Education, Science, Technology, Sport and Culture, Japan, and the Venture Business Laboratory, Yamaguchi University, for M.K. and T.W.I.; by the Deutsche Forschungsgemeinschaft (Grant No. Bu 450/6-3) and the Fonds der Chemischen Industrie for J.P.G., G.H., and R.J.B.; and by NASA Grant Nos. NAG-9088 and NAG5-11453 for J.G.W. and P.C.S.

[1] D. P'equignot, S.M. Aldrovandi, and G. Stasinska, Astron. Astrophys. **63**, 313 (1978); also see *Molecular Astrophysics*, edited by T.W. Hartquist (Cambridge University Press, Cambridge, 1990).
[2] H.C. Suk, A. Guilbaud, and B. Hird, J. Phys. B **11**, 1465 (1978).
[3] E.W.P. Bloemen, D. Dijkkamp, and F.J. de Heer, J. Phys. B **15**, 1391 (1982).
[4] K. Okuno and Y. Kaneko, Abstracts of XIII ICPEAC, Berlin, 1983 (unpublished), p. 543.
[5] T. Kusakabe, N. Nagai, H. Hanaki, T. Horiuchi, and M. Sakisaka, J. Phys. Soc. Jpn. **52**, 4122 (1983).
[6] I.P. Flaks and E.S. Solov'ev, Sov. Phys. Tech. Phys. **3**, 577 (1958).
[7] E. Mercier, G. Chambaud, and B. Levy, J. Phys. B **18**, 3591 (1985).
[8] I. Ben-Itzhak, J.P. Bouhnik, Z. Chen, B.D. Esry, I. Gertner, C. Heinemann, W. Kock, C.D. Lin, and B. Rosner, Phys. Rev. A **56**, 1268 (1997).
[9] M. Kimura, J.P. Gu, Y. Li, G. Hirsch, and R.J. Buenker, Phys. Rev. A **49**, 3131 (1994).
[10] R.J. Buenker and S.D. Peyerimhoff, Theor. Chim. Acta **35**, 33 (1974); *ibid.* **39**, 217 (1975); R.J. Buenker, Int. J. Quantum Chem. **29**, 435 (1986); S. Krebs and R.J. Buenker, J. Chem. Phys. **103**, 5613 (1995).
[11] R.J. Buenker, in *Proceedings of the Workshop on Quantum Chemistry and Molecular Physics, Wollongong, Australia*, edited by P.G. Burton (University Press, Wollongong, 1980); in *Studies in Physical and Theoretical Chemistry*, edited by R. Carbo (Elsevier, Amsterdam, 1981), Vol. 21, p. 17; R.J. Buenker and R.A. Phillips, J. Mol. Struct.: THEOCHEM **123**, 291 (1985).
[12] G. Hirsch, P.J. Bruna, R.J. Buenker, and S.D. Peyerimhoff, Chem. Phys. **45**, 335 (1980).
[13] T.H. Dunning, Jr., J. Chem. Phys. **90**, 1007 (1989).
[14] J. Roemelt, S.D. Peyerimhoff, and R.J. Buenker, Chem. Phys. **34**, 403 (1978).
[15] M. Kimura and N.F. Lane, Adv. At., Mol., Opt. Phys **26**, 79 (1989).
[16] P.C. Stancil, N.J. Clarke, B. Zygelman, and D.L. Cooper, J. Phys. B **32**, 1523 (1999).
[17] R. Suzuki, A. Watanabe, H. Sato, J.P. Gu, G. Hirsch, R.J. Buenker, M. Kimura, and P.C. Stancil, Phys. Rev. A **63**, 042717 (2001).
[18] A. R. Turner, D. L. Cooper, J. G. Wang, and P. C. Stancil, Phys. Rev. A **68**, 012704 (2003).